Original Article | Neuroimaging and Head & Neck

https://doi.org/10.3348/kjr.2018.19.3.452
pISSN 1229-6929 · eISSN 2005-8330
Korean J Radiol 2018;19(3):452-462

Korean Journal of Radiology
KJR

Brain Regional Homogeneity Changes in Cirrhotic Patients with or without Hepatic Encephalopathy Revealed by Multi-Frequency Bands Analysis Based on Resting-State Functional MRI

Gaoyan Zhang, PhD[1], Yue Cheng, PhD[2], Wen Shen, PhD[2], Baolin Liu, PhD[1, 3], Lixiang Huang, MD[2], Shuangshuang Xie, MD[2]

[1]Tianjin Key Laboratory of Cognitive Computing and Application, School of Computer Science and Technology, Tianjin University, Tianjin 300350, China; [2]Department of Radiology, Tianjin First Central Hospital, Tianjin 300192, China; [3]State Key Laboratory of Intelligent Technology and Systems, National Laboratory for Information Science and Technology, Tsinghua University, Beijing 100084, China

Objective: To investigate brain regional homogeneity (ReHo) changes of multiple sub-frequency bands in cirrhotic patients with or without hepatic encephalopathy using resting-state functional MRI.

Materials and Methods: This study recruited 46 cirrhotic patients without clinical hepatic encephalopathy (noHE), 38 cirrhotic patients with clinical hepatic encephalopathy (HE), and 37 healthy volunteers. ReHo differences were analyzed in slow-5 (0.010–0.027 Hz), slow-4 (0.027–0.073 Hz), and slow-3 (0.073–0.198 Hz) bands. Routine analysis of (0.010–0.080 Hz) band was used as a benchmark. Associations of abnormal ReHo values in each frequency band with neuropsychological scores and blood ammonia level were analyzed. Pattern classification analyses were conducted to determine whether ReHo differences in each band could differentiate the three groups of subjects (patients with or without hepatic encephalopathy and healthy controls).

Results: Compared to routine analysis, more differences between HE and noHE were observed in slow-5 and slow-4 bands ($p < 0.005$, cluster > 12, overall corrected $p < 0.05$). Sub-frequency band analysis also showed that ReHo abnormalities were frequency-dependent (overall corrected $p < 0.05$). In addition, ReHo abnormalities in each sub-band were correlated with blood ammonia level and neuropsychological scores, especially in the left inferior parietal lobe (overall corrected $p < 0.05$ for all frequency bands). Pattern classification analysis demonstrated that ReHo differences in lower slow-5 and slow-4 bands (both $p < 0.05$) and higher slow-3 band could differentiate the three groups ($p < 0.05$). Compared to routine analysis, ReHo features in slow-4 band obtained better classification accuracy (89%).

Conclusion: Cirrhotic patients showed frequency-dependent changes in ReHo. Sub-frequency band analysis is important for understanding HE and clinical monitoring.

Keywords: *Hepatic encephalopathy; Frequency-dependent; Regional homogeneity (ReHo); Resting-state functional MRI; Brain; Liver cirrhosis*

Received May 20, 2017; accepted after revision November 23, 2017.
This study was supported by the Peiyang Scholar Program of Tianjin University (No. 2018XRG-0037) and the National Natural Science Foundation of China (No. 81601482 and No. 61571327).

Corresponding author: Yue Cheng, PhD, Department of Radiology, Tianjin First Central Hospital, Fukang Road No.24, Nankai District, Tianjin 300192, China.
• Tel: (86) 13821559069 • Fax: (86) 22-23361365
• E-mail: chengyue200017076@163.com

INTRODUCTION

Cirrhotic patients are characterized by a wide range of neuropsychiatric abnormalities, including personality disorders and inappropriate affective, behavioral, and sleep disturbances (1). Episodes of hepatic encephalopathy are associated with poor prognosis of cirrhotic patients (2, 3). Clinical spectrum of hepatic encephalopathy includes mild cognitive impairment, coma, and even death (4). Brain dysfunction in cirrhotic patients with or without hepatic encephalopathy has not been fully understood yet. Thus, it is difficult to predict disease development in such patients.

Korean Journal of Radiology
KJR

Failure rate of therapy remains high for cirrhotic patients.

Previously, many researchers have used resting-state functional MRI (fMRI) to investigate abnormality in brain function because of its feasibility compared to task-state fMRI (5). For instance, some studies have reported alterations in amplitude of low-frequency fluctuation of intrinsic brain activity in different types of cirrhotic patients and changes after liver transplantation (6-8). By analyzing functional connectivity in the brain, some researchers have observed impaired small-world network efficiency and functional connectivity network in cirrhotic patients (1, 9, 10). Some studies have also analyzed regional homogeneity (ReHo) using resting-state fMRI and found abnormality in intra-regional synchronization in cirrhotic patients with or without overt hepatic encephalopathy (11, 12). Although existing resting-state fMRI studies provide some insights into brain dysfunction of cirrhotic patients, they have mainly focused on brain activities in a fixed frequency band (0.01–0.08 Hz). Whether resting-state human brain function in different frequency bands is altered to the same extent in cirrhotic patients is currently unknown. It has been suggested that blood oxygenation level-dependent (BOLD) oscillation frequency of a single voxel, and regional synchrony of this single voxel with several neighboring voxels may not be independent of each other in human brain at resting-state (13), which means that regional synchrony may be frequency-dependent. Some studies have suggested that distinct or invariant topological patterns are distributed in various frequency intervals (14, 15). It has been hypothesized that frequency-dependent effects in different brain regions reflect synaptic, functional, or cytoarchitectonic characteristics (16, 17). They might be affected by the progression of cognitive impairment (18).

Therefore, the objective of this study was to determine frequency-dependent ReHo changes in cirrhotic patients with or without clinical hepatic encephalopathy (HE or noHE) and whether these frequency-specific changes could be used to differentiate HE, noHE, and healthy controls (HCs). Previous studies have decomposed low frequency BOLD signals into four different frequency bands according to neuronal oscillations in cortical networks (15, 19). In this study, we mainly focused on slow-5 (0.010–0.027 Hz), slow-4 (0.027–0.073 Hz), and slow-3 (0.073–0.198 Hz) bands because signal of slow-6 (0–0.010 Hz) band primarily reflected very low frequency drift (15). We believe that mapping brain alterations of cirrhotic patients in multiple frequency bands is of great clinical interest as it can provide more details of brain dysfunctions that are important for monitoring disease development and response to therapy.

MATERIALS AND METHODS

Participants

This study was approved by the local Medical Research Ethics Committee. Informed consent was obtained from each subject before participating in this study.

A total of 130 subjects were recruited for this study. Patients were excluded if they took psychotropic medications, suffered from uncontrolled endocrine disorders, had other neuropsychiatric disorders or metabolic diseases, had alcohol abuse within 6 months prior to the study, or had large head motions during scanning. After exclusions, 121 subjects remained, including 46 noHE, 38 HE, and 37 healthy volunteers matched by age, sex, and educational level for the HC group (Table 1). Cirrhotic patients were diagnosed according to case history, laboratory tests, and imaging findings. The severity of liver disease was assessed by calculating the Child-Pugh score (20). Hepatic encephalopathy patients were graded based on the West Haven criteria (21).

A day before MRI scanning, the following laboratory tests were carried out. For each cirrhotic patient, venous blood ammonia level, prothrombin time, total bilirubin level, and albumin level were determined. Neuropsychological examinations including number connection of type A (NCT-A) and digit-symbol test (DST) were conducted for both patients and normal controls. DST was used to evaluate attention and visual memory ability while NCT-A was used to examine psychomotor speed (22). Test data are summarized in Table 1.

MRI Data Collection

All participants were scanned using a Siemens 3T MRI scanner (TIM-Trio; Siemens Medical Solutions, Erlangen, Germany) with a 32-channel head coil. Foam padding was used to reduce head motion. During resting-state fMRI scanning, each participant was instructed to stay awake with eyes closed and not to think of anything particularly. Two-dimensional T2-weighted turbo spin echo and T1-weighted fast low-angle shot sequences were used to detect brain lesions. Gradient echo-planar imaging sequence was used to acquire BOLD images with the following parameters: measurement = 200, echo time = 30 ms, repetition time = 2500 ms, flip angle = 90°, field of view = 220 x 220 mm,

matrix = 96 x 96, slice thickness = 3 mm, slice gap = 0.3 mm, and number of slices = 40.

Data Preprocessing

MRI data were preprocessed using Data Processing and Analysis of Brain Imaging toolbox (23) embedded in MATLAB 2013a (MathWorks, Natick, MA, USA). Before processing, the first 10 volumes were removed to account for T1 equilibrium effect. Acquisition time and head motion were corrected for the remaining 190 volumes. Subjects with translational or rotational parameters exceeding 2 mm or 2° were removed. Furthermore, frame-wise displacement was calculated based on a previous study (24) to control head motion in each group (Table 1). One-way analysis of variance showed no significant differences in frame-wise displacement among the three groups (p = 0.964). Linear trend of BOLD signal was then removed and nuisance covariates including cerebrospinal fluid signals, white matter signals, global signals, and head motion parameters were regressed out to further reduce confounding factor effects. After this, co-registration, segmentation, and writing normalization were conducted using unified segmentation of each participant's T1 image. Normalized volumes were resampled to 3 x 3 x 3 mm^3. Normalized data were then band-pass filtered in three frequency bands (0.010–0.027 Hz, 0.027–0.073 Hz, and 0.073–0.198 Hz), respectively. Routine analysis for band of 0.010–0.080 Hz was also carried out as a standard benchmark. Spatial smoothing could enhance the ReHo value artificially and reduce the reliability (25). Therefore, spatial smoothing was performed in this study after ReHo analysis.

Individual and Group ReHo Analysis in Separate Frequency Bands

For filtered data in each band, whole-brain ReHo analysis was performed for each participant by calculating Kendall's coefficient of concordance between time series of a given voxel and those of its nearest 26 voxels (26). For standardization, individual ReHo map was transformed to a Z-map by subtracting mean ReHo value in the whole brain and then dividing by the standard deviation. Spatial smoothing was performed using a Gaussian kernel with full width at the half maximum of 4 mm.

To calculate frequency-specific ReHo differences, one-way analysis of covariance (ANCOVA) with group (HE, noHE, and HC) as a main factor was conducted in each frequency band. Age, sex, educational level, and head motion parameters were used as covariates. Furthermore, two-sample t test was performed to compare between-group differences. Two-sample t tests among groups in the frequency band of 0.010–0.080 Hz were also conducted for comparison. In all analyses, individual p value was set at 0.005 with a cluster size of 12 under a whole-brain mask. The significance of multiple comparisons was corrected using AFNI AlphaSim

Table 1. Demographic, Neuropsychological and Clinical Data

Protocols	HC (n = 37)	noHE (n = 46)	HE (n = 38)	*P*
Sex (male/female)	25/12	27/19	27/11	0.467*
Age (years)	50.6 ± 7.4	50.8 ± 8.3	50.3 ± 8.6	0.952†
Education (years)	12.8 ± 2.8	11.7 ± 3.6	11.6 ± 3.4	0.195†
Frame-wise displacement	0.08 ± 0.05	0.08 ± 0.04	0.08 ± 0.05	0.964†
NCT-A (seconds)	42.0 ± 10.2	71.0 ± 34.5	76.5 ± 37.3	< 0.001‡
				< 0.001§
				0.487‖
DST (score)	48.9 ± 9.7	33.8 ± 15.1	29.4 ± 14.4	< 0.001‡
				< 0.001§
				0.177‖
Blood ammonia (μmol/L)	-	62.8 ± 25.8	85.0 ± 32.8	0.001‖
Albumin (mg/dL)	-	30.7 ± 7.7	31.5 ± 6.2	0.569‖
Total bilirubin (mg/dL)	-	83.2 ± 108.4	78.5 ± 125.0	0.857‖
Prothrombin time (seconds)	-	18.0 ± 6.5	17.0 ± 4.5	0.393‖
Child-Pugh A/B/C	-	4/17/25	0/11/27	-

Data are presented as mean ± standard deviation. *Pearson χ^2 test of three groups (two-tailed), †One-way analysis of variance test among three groups (two-tailed), ‡Two-sample t test between noHE and HC groups (two-tailed), §Two-sample t test between HE and HC groups (two-tailed), ‖Two-sample t test between HE and noHE groups (two-tailed). DST = digit-symbol test, HC = healthy control, HE = cirrhotic patients with clinical hepatic encephalopathy, NCT-A = number connection test of type A, noHE = cirrhotic patients without clinical hepatic encephalopathy

Korean Journal of Radiology
KJR

program (http://afni.nimh.nih.gov/pub/dist/doc/manual/AlphaSim.pdf) at overall $p < 0.05$.

Associations of Frequency-Specific ReHo Abnormality with Neuropsychological Performance and Blood Ammonia Level

To evaluate the relationship of abnormal ReHo values in each frequency band with neuropsychological performance and blood ammonia level, partial correlation analyses of data in patient groups were conducted with age, sex, educational level, and head motion parameters as covariates. The significance was analyzed within a mask generated by one-way ANCOVA under each frequency band. Individual p value was set at 0.005 with cluster sizes of 11 for slow-5 band, 10 for slow-4 band, 10 for slow-3 band, and 12 for band of 0.010–0.080 Hz. Multiple comparisons were corrected using the AlphaSim procedure at an overall $p < 0.05$ as described above.

Multi-Voxel Pattern Classification Analysis Based on Frequency-Specific ReHo Features

To further determine whether abnormal ReHo values in each frequency band could differentiate different groups, a multi-voxel pattern classification analysis was conducted. A leave-one-out cross-validation method was applied to train the classifier. In each cross-validation trial, K-1 training samples under the ANCOVA map were defined as input data. An F-score method for calculating between-group difference of voxels was used to select features. Support vector machine method was used as the classifier. Accuracy, sensitivity, and specificity were calculated based on the mixture matrix. Significance of the classification result was evaluated using a permutation test by random permutation of class labels 1000 times. Whether the classification result was obtained by chance was then determined. Moreover, classification analysis based on ReHo values obtained in routine analysis (0.010–0.080 Hz) was also conducted to compare classification accuracies.

RESULTS

Frequency-Specific Group ReHo Differences

Results of one-way ANCOVAs of ReHo values among the three groups in each sub-frequency band are shown in Figure 1 and Table 2. Results of two-sample t tests of between-group ReHo differences in each sub-frequency band are shown in Figure 2B-D. Results of between-group ReHo differences in routine 0.010–0.080 Hz are shown in Figure 2A as a benchmark.

In the slow-5 frequency band, group differences in ReHo were mainly located in motor-related areas (bilateral precentral/postcentral gyrus, left superior frontal gyrus/middle frontal gyrus [SFG/MFG]), visuospatial processing-related areas (precuneus, superior parietal lobe [SPL], superior occipital gyrus [SOG], bilateral lingual gyrus [LG]), default mode network (DMN) regions (inferior parietal lobe [IPL], supramarginal gyrus [SMG], angular gyrus [AG], posterior cingulate cortex [PCC], anterior cingulate cortex/medial prefrontal cortex [ACC/MPFC], right middle temporal gyrus/superior temporal gyrus/inferior temporal gyrus [MTG/STG/ITG], and rectus), subcortical regions (right thalamus, right caudate), and the bilateral cerebellum (individual $p < 0.005$, cluster > 12, overall $p < 0.05$) (Fig. 1A).

In the slow-4 frequency band, regions that showed group differences were similar to those in the slow-5 band. However, brain cluster was wider in the slow-4 band. In

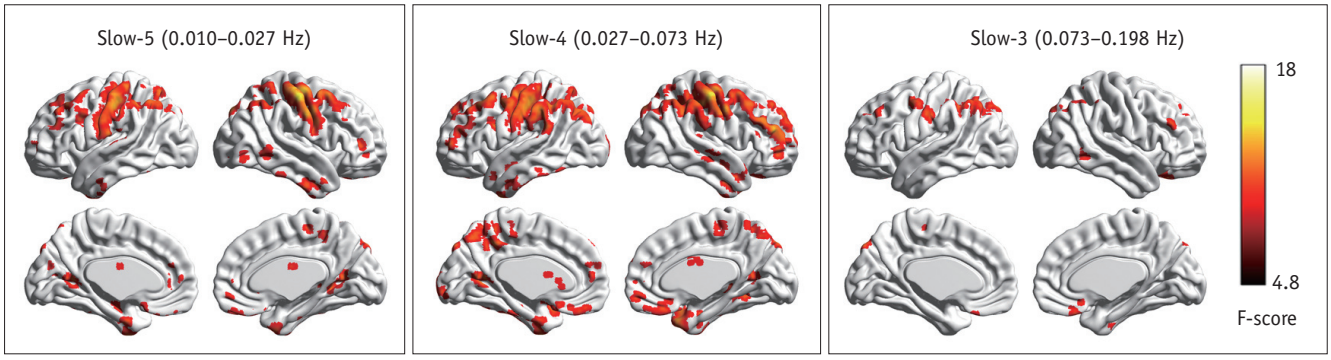

Fig. 1. Regional homogeneity change pattern across frequency bands.
A. One-way ANCOVA result in slow-5 frequency band. **B.** One-way ANCOVA result in slow-4 frequency band. **C.** One-way ANCOVA result in slow-3 frequency band. ANCOVA = analysis of covariance

Table 2. Regions Showing Significant Group Changes in Regional Homogeneity in Slow-5, Slow-4, and Slow-3 Frequency Bands (AlphaSim Corrected, Overall $p < 0.05$)

Brain Clusters	Number of Voxels	Brodmann Area	MNI Coordinates			Peak F-Value
			x	y	z	
Slow-5 (0.010–0.027 Hz)						
L. cerebellum	32		-18	-66	-45	8.45
R. cerebellum	237		33	-54	-36	11.00
R. FG/MTP	31	38	21	9	-45	9.15
R. STG	21	13/41	39	-18	-9	9.98
R. IOG/ITG	26	19	60	-69	-9	9.40
L. ACC/MPFC	52	32/10	0	45	3	8.60
R. caudate	35		9	18	0	7.94
R. calcarine	64	30	18	-51	3	9.24
L. calcarine	49	30	-12	-57	6	10.01
R. thalamus	78		18	-9	6	10.28
L. MFG	24	10	-33	60	6	7.74
L. SOG	27	18	-12	-78	21	8.81
L. postcentral/precentral gyrus/IPL/SPL/SMG/AG	908	40/3/4/7	-48	-18	54	14.80
R. postcentral/precentral gyrus/IPL/SPL/AG	955	3/6/40/7	54	-18	54	22.98
L. DLPFC	27	46	-45	42	27	9.68
L. MFG	139	8	-36	27	48	10.13
Slow-4 (0.027–0.073 Hz)						
R/L. cerebellum	1263		33	-57	-39	13.67
L. STP/ITG/MTG	134	20/38/21	-45	12	-21	9.88
R. rectus	31	11	3	30	-24	6.66
R. OSFG	28	47	15	27	-30	9.32
L. OIFG	23	47	-18	18	-24	7.70
R. MTG/STG	30	21	72	-18	-6	7.43
R. thalamus/caudate	102		18	-12	3	11.06
L. ACC/SFG	48	9/10/32	0	51	28	10.96
L. calcarine	72	30	-12	-60	9	12.63
R. calcarine	22	30	21	-57	12	7.97
L. postcentral/precentral gyrus/IPL/MFG/SMG/AG/precuneus/SFG/SPL/MOG	1434	40/6/3/8/2/4/7/9/19/39	-48	-15	54	16.66
R. postcentral/precentral gyrus/MFG/SFG/IPL/AG/SMG/SPL	1457	3/40/6/3/9/46/10/8/4	54	-18	54	22.60
L. precuneus	25	7	9	-69	51	7.14
Slow-3 (0.073–0.198 Hz)						
R. cerebellum	61		3	-75	-48	11.51
L. cerebellum	124		-48	-51	-48	8.70
R. OIFG/OSFG/rectus	62	11/25	9	30	-27	8.67
L. caudate	37		-12	-9	21	11.29
L. postcentral/precentral gyrus	69	3/4	-57	-18	33	7.79
R. MFG	27	9	54	24	36	7.60
L. SOG/IPL/AG/SPL	365	40/7/39/19	-18	-87	45	9.98
R. SFG/MFG	26	9/8	24	48	45	7.22
L. MFG/SFG	25	9/8	-36	39	42	8.18
R. SOG/SPL/AG	34	7	21	-84	42	8.52
R. SPL/IPL/AG	95	40/7	39	-60	63	10.59

ACC = anterior cingulate cortex, AG = angular gyrus, DLPFC = dorsal lateral prefrontal gyrus, FG = fusiform gyrus, IOG = inferior occipital gyrus, IPL = inferior parietal lobe, ITG = inferior temporal gyrus, L = left side, MFG = middle frontal gyrus, MNI = Montreal Neurological Institute, MOG = middle occipital gyrus, MPFC = medial prefrontal cortex, MTG = middle temporal gyrus, MTP = middle temporal pole, OIFG = orbital inferior frontal gyrus, OSFG = orbital superior frontal gyrus, R = right side, SFG = superior frontal gyrus, SMG = supramarginal gyrus, SOG = superior occipital gyrus, SPL = superior parietal lobe, STG = superior temporal gyrus, STP = superior temporal pole

Korean Journal of Radiology
KJR

addition, the bilateral prefrontal cortex, left STG, ITG, and superior temporal pole showed significant group differences in the slow-4 band, but not in the slow-5 band (individual $p < 0.005$, cluster > 12, overall $p < 0.05$) (Fig. 1B).

In comparison, group-difference regions in the slow-3 frequency band were significantly fewer than those in slow-4 or slow-5 frequency band. These regions were located in the bilateral SPL/IPL/AG, bilateral SOG, bilateral MFG/

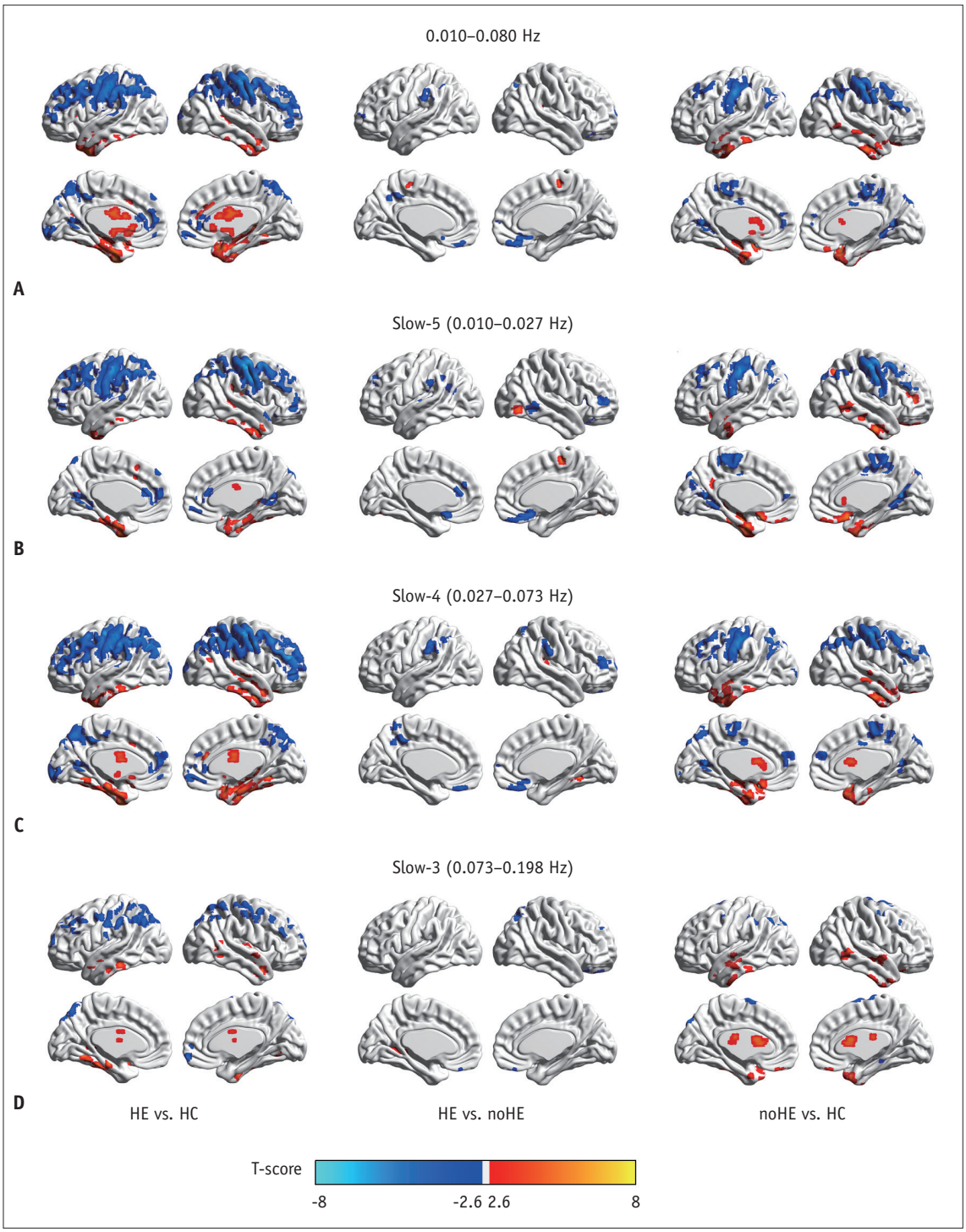

Fig. 2. Between-group regional homogeneity differences in routine analysis and in sub-frequency band analysis.
A. Two-sample *t* test result in 0.010–0.080 Hz. **B.** Two-sample *t* test result in slow-5 frequency band. **C.** Two-sample *t* test result in slow-4 frequency band. **D.** Two-sample *t* test result in slow-3 frequency band. HC = healthy control, HE = cirrhotic patients with clinical hepatic encephalopathy, noHE = cirrhotic patients without clinical hepatic encephalopathy

SFG, left postcentral/precentral gyrus, left caudate, right ITG, right rectus, and bilateral cerebellum (individual p < 0.005, cluster > 12, overall p < 0.05) (Fig. 1C). Conjunction analysis revealed consistent group differences in these three bands in bilateral IPL/SPL/AG, left postcentral gyrus, and right cerebellum (individual p < 0.005, cluster > 12, overall p < 0.05).

Two-sample t tests in each band showed widespread differences in ReHo between HE and HC groups, fewer differences in the comparison between noHE and HC groups, and the fewest differences between HE and noHE groups (individual p < 0.005, cluster > 12, overall p < 0.05) (Fig. 2).

Compared with benchmark result in 0.010–0.080 Hz (individual p < 0.005, cluster > 12, overall p < 0.05) (Fig. 2A), frequency-specific ReHo analysis showed similar spatial location of difference regions in the comparison of HE with HC or noHE with HC, demonstrating reliability of these results. Interestingly, more ReHo differences (such as those in the right IPL, right SFG, and right occipital gyrus) were observed in the comparison of HE with noHE in slow-5 and slow-4 bands. Sub-frequency band analysis also showed that ReHo differences such as those for some regions in DMN (precuneus/PCC, MPFC, bilateral IPL) and subcortical cortex were frequency-dependent.

Correlation Results of Frequency-Specific ReHo Abnormality with Neuropsychological Performance and Ammonia Level

Figure 3A shows correlation maps of ReHo abnormality in 0.010–0.080 Hz with DST, NCT-A values, and ammonia level (individual p < 0.005, cluster > 12, overall p < 0.05). Figure 3B-D displays corresponding correlation maps in sub-frequency bands. It can be seen that correlation regions in these two different analysis methods are basically consistent except that these correlation regions are frequency-dependent in sub-frequency band analysis.

Figure 3B shows correlation maps in slow-5 band (individual p < 0.005, cluster > 11, overall p < 0.05). It could be clearly seen that ReHo values in the right LG, the right precentral/postcentral gyrus, and the left IPL were positively correlated with DST score while ReHo values in the right ITG and the bilateral cerebellum were negatively correlated with DST score. Only ReHo values in the left SOG and the left IPL/AG showed negative correlations with NCT-A score. Abnormal ReHo values in the left MFG, and the left IPL were negatively correlated with blood ammonia level.

Figure 3C illustrates correlation maps in slow-4 band (individual p < 0.005, cluster > 10, overall p < 0.05). ReHo values in the bilateral cerebellum and the left ITG had negative correlations with DST score. However, ReHo values in the bilateral IPL, the left SOG, the right MFG, and the left postcentral gyrus showed positive correlations with DST score. For correlations with NCT-A, negative correlations were observed in the right orbital middle frontal gyrus, the right MFG, the left postcentral gyrus, and the left IPL/AG/SMG/middle occipital gyrus (MOG) whereas positive correlations were observed in the right caudate and the bilateral cerebellum. For correlations with ammonia level, there were negative correlations in the left AG/IPL, the left IPL/MOG/AG, the left calcarine and the left SMG but positive correlations in the bilateral cerebellum.

Figure 3D illustrates correlation maps in slow-3 band (individual p < 0.005, cluster > 10, overall p < 0.05). Regions in bilateral IPL/AG/SPL, the left SOG, and the left MFG showed positive correlations with DST score. Only ReHo values in the left SOG and the left IPL/AG showed negative correlations with NCT-A values. For correlations with ammonia level, negative correlations were observed in the right SFG/MFG and the left IPL/AG/SPL/SOG.

Pattern Classification Results Based on Frequency-Specific ReHo Features

Classification accuracies, sensitivity, and specificity of three discriminant analyses (HE vs. HC, HE vs. noHE, noHE vs. HC) are summarized in Table 3. All these classification accuracies were significant based on permutation test (p < 0.05). ReHo differences in each frequency band could significantly differentiate the three groups. Compared to classification accuracies based on ReHo features in 0.010–0.080 Hz (benchmark result), classification accuracies were higher when using ReHo features in slow-4 band were used. Moreover, compared to classification accuracies in benchmark result, classification of HE with noHE were higher in both slow-5 and slow-4 bands (Table 3), consistent with earlier results showing much more ReHo differences in these two bands (Fig. 2B, C).

DISCUSSION

The current study analyzed brain ReHo values in multiple sub-frequency bands to investigate frequency-specific ReHo changes in HE or noHE. Through group statistical comparison, clinical correlation analysis, pattern classification analysis, and comparisons with benchmark

Korean Journal of Radiology
KJR

result, our results showed benefits of sub-frequency band analysis and frequency-dependent characteristic of ReHo changes in cirrhotic patients.

Frequency-Specific Group ReHo Differences

In all three bands, there were more changes of ReHo values in cirrhotic patients with hepatic encephalopathy than those in patients without hepatic encephalopathy, especially in prefrontal regions, MTG, IPL, and precuneus

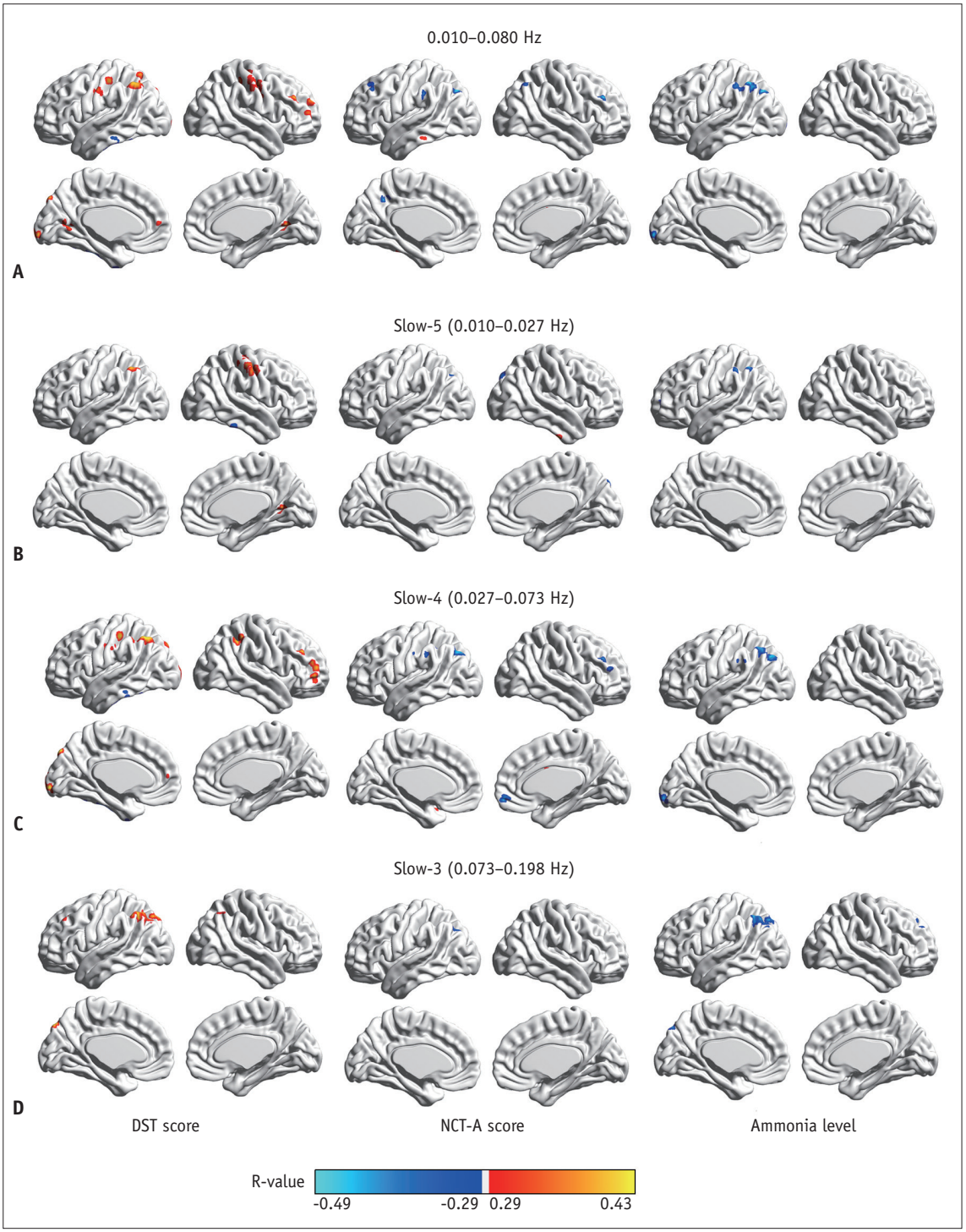

Fig. 3. Correlation of regional homogeneity values in group-difference regions with DST, NCT-A scores, and blood ammonia level. **A.** Correlation map in 0.010–0.080 Hz. **B.** Correlation map in slow-5 band. **C.** Correlation map in slow-4 band. **D.** Correlation map in slow-3 band. DST = digit-symbol test, NCT-A = number connection test of type A

Table 3. Accuracy, Sensitivity, and Specificity of Pattern Classification Analysis Using between-Group Regional Homogeneity Difference Features in Different Frequency Bands

Indices	HE vs. HC	HE vs. noHE	noHE vs. HC
Routine band (0.010–0.080 Hz)			
Accuracy	0.87	0.81	0.80
Sensitivity	0.84	0.78	0.79
Specificity	0.89	0.84	0.80
Slow-5 (0.010–0.027 Hz)			
Accuracy	0.87	0.83	0.78
Sensitivity	0.89	0.74	0.76
Specificity	0.84	0.91	0.80
Slow-4 (0.027–0.073 Hz)			
Accuracy	0.89	0.83	0.83
Sensitivity	0.89	0.84	0.81
Specificity	0.89	0.83	0.85
Slow-3 (0.073–0.198 Hz)			
Accuracy	0.76	0.77	0.81
Sensitivity	0.76	0.71	0.76
Specificity	0.76	0.83	0.85

(Fig. 1). These abnormal regions are similar to results of our previous study using functional connectivity density (FCD) metric (9). In slow-5 and slow-4 frequency bands, group differences were distributed in widespread cortical regions. However, these differences were observed in limited brain areas in the higher slow-3 frequency band. Such differentially affected ReHo in different bands might be due to the possibility that frequency-specific ReHo signature is constrained by cytoarchitecture, synaptic types, and neurovascular properties of the local brain tissue as suggested in a previous study (13). Comparing these three bands, it is clear that ReHo changes in DMN regions are significant in slow-5 and slow-4 bands compared to those in slow-3 band. Such frequency-dependent group ReHo differences in DMN regions are in line with results of a previous study showing that BOLD oscillations in DMN regions are frequency-dependent (17). Interestingly, the bilateral SPL/IPL/AG, left postcentral gyrus, and right cerebellum showed consistent group changes in ReHo values across frequency bands. It has been shown that lower frequency fluctuations coordinate long-distance neural activity while higher frequency fluctuations coordinate more local neural activity (17, 19). Therefore, we can infer that the long-distance or short-distance functional coordination might be impaired in these regions in cirrhotic patients. A recent FCD study has shown that the bilateral IPL exhibits altered long-distance FCD and the left postcentral gyrus exhibits changes in local FCD in cirrhotic patients with minimal HE (27), consistent with our inference.

Compared to routine analysis within 0.010–0.080 Hz, similar abnormal distribution in frequency-specific analysis demonstrates the reliability of our results. More abnormal regions in the comparison between HE and noHE in slow-5 and slow-4 bands and frequency-dependent ReHo change patterns demonstrate the benefit of sub-frequency band analysis.

Clinical Correlations of Frequency-Specific ReHo Changes

To clearly understand the relationship between ReHo and disease severity, we cascaded HE and noHE groups together in the correlation analysis. It is known that higher DST scores represent better attention and visual memory ability in cirrhotic patients. Positive correlations of fronto-parietal regions and occipital regions with DST values found in this study are consistent with important roles of these regions in attention and visual memory function (28). Moreover, longer completion times in the NCT-A test represent worse psychomotor speeds. Thus, negative correlations of ReHo in motor-related areas (postcentral gyrus, caudate, and cerebellum) with NCT-A scores observed in our study were in our anticipation. Significant negative correlations of left IPL/AG and cerebellum with blood ammonia level found in this study were consistent with our recent study on a smaller patient groups using FCD metric (9). However, correlation regions were different in different frequency bands, suggesting frequency-specific ReHo markers for monitoring HE performance. Comparing all three bands, we could see a significant correlation in left IPL, demonstrating the important role of this region in HE (9, 27). Specifically, comparing correlation maps in the three frequency bands, majority of correlated regions were clearly found in the slow-4 band, demonstrating that the slow-4 band might contribute more to abnormality in HE patients. The highest classification accuracy with ReHo features in the slow-4 band further supports this inference. Compared with classification accuracy based on ReHo features in 0.010–0.080 Hz, the higher accuracy based on features in the slow-4 band also suggests the clinical benefit of sub-frequency band analysis. Moreover, ReHo values in the slow-3 band not analyzed in routine resting-state fMRI analysis showed significant correlations with lab test scores. ReHo features in slow-3 frequency band could also be used to differentiate the three groups. Thus, future studies should also pay attention to this higher frequency band.

Korean Journal of Radiology
KJR

Limitations and Future Considerations

Some limitations of this study should be mentioned. First, only two neuropsychological tests were used. A broader spectrum of tests can better evaluate various cognitive domains of cirrhotic patients. Second, patients used in this study had heterogeneous etiologies that might limit comprehensive interpretation of our results. Third, due to difficulty of data collection, we could only observe the progression from noHE to HE in different subjects. A longitudinal study in the same patient group would provide more persuasive results. In future studies, these limitations should be fully considered to further verify findings of this study.

Conclusion

Analyses of ReHo in multiple sub-frequency bands showed that most abnormal ReHo values in cirrhotic patients were found in slow-5 and slow-4 bands. Among the three bands, ReHo changes in slow-4 band showed the highest correlations with neuropsychological performance and blood ammonia level and differentiated the three groups with the highest accuracy. Compared with benchmark result, sub-frequency band analysis showed more ReHo changes in the comparison between HE and noHE and higher classification accuracy based on features in slow-4 band. Although there were limited regions with ReHo changes in slow-3 band, these changes could also discriminate the three different groups, demonstrating that future studies should pay attention to this band. In conclusion, results in this study extend our knowledge of altered brain ReHo patterns at resting state in cirrhotic patients. In the future, more attention should be paid to frequency-specific property to have an overall view on this disease.

REFERENCES

1. Hsu TW, Wu CW, Cheng YF, Chen HL, Lu CH, Cho KH, et al. Impaired small-world network efficiency and dynamic functional distribution in patients with cirrhosis. *PLoS One* 2012;7:e35266
2. Alonso J, Córdoba J, Rovira A. Brain magnetic resonance in hepatic encephalopathy. *Semin Ultrasound CT MR* 2014;35:136-152
3. Cheng Y, Zhang G, Shen W, Huang LX, Zhang L, Xie SS, et al. Impact of previous episodes of hepatic encephalopathy on short-term brain function recovery after liver transplantation: a functional connectivity strength study. *Metab Brain Dis* 2018;33:237-249
4. McPhail MJ, Patel NR, Taylor-Robinson SD. Brain imaging and hepatic encephalopathy. *Clin Liver Dis* 2012;16:57-72
5. Park SH, Han PK, Choi SH. Physiological and functional magnetic resonance imaging using balanced steady-state free precession. *Korean J Radiol* 2015;16:550-559
6. Lv XF, Ye M, Han LJ, Zhang XL, Cai PQ, Jiang GH, et al. Abnormal baseline brain activity in patients with HBV-related cirrhosis without overt hepatic encephalopathy revealed by resting-state functional MRI. *Metab Brain Dis* 2013;28:485-492
7. Chen HJ, Zhu XQ, Jiao Y, Li PC, Wang Y, Teng GJ. Abnormal baseline brain activity in low-grade hepatic encephalopathy: a resting-state fMRI study. *J Neurol Sci* 2012;318:140-145
8. Zhang G, Cheng Y, Shen W, Liu B, Huang L, Xie S. The short-term effect of liver transplantation on the low-frequency fluctuation of brain activity in cirrhotic patients with and without overt hepatic encephalopathy. *Brain Imaging Behav* 2017;11:1849-1861
9. Zhang G, Cheng Y, Liu B. Abnormalities of voxel-based whole-brain functional connectivity patterns predict the progression of hepatic encephalopathy. *Brain Imaging Behav* 2017;11:784-796
10. Chen HJ, Zhu XQ, Shu H, Yang M, Zhang Y, Ding J, et al. Structural and functional cerebral impairments in cirrhotic patients with a history of overt hepatic encephalopathy. *Eur J Radiol* 2012;81:2463-2469
11. Lv XF, Qiu YW, Tian JZ, Xie CM, Han LJ, Su HH, et al. Abnormal regional homogeneity of resting-state brain activity in patients with HBV-related cirrhosis without overt hepatic encephalopathy. *Liver Int* 2013;33:375-383
12. Lin WC, Hsu TW, Chen CL, Lu CH, Chen HL, Cheng YF. Resting state-fMRI with ReHo analysis as a non-invasive modality for the prognosis of cirrhotic patients with overt hepatic encephalopathy. *PLoS One* 2015;10:e0126834
13. Song X, Zhou S, Zhang Y, Liu Y, Zhu H, Gao JH. Frequency-dependent modulation of regional synchrony in the human brain by eyes open and eyes closed resting-states. *PLoS One* 2015;10:e0141507
14. Qian L, Zhang Y, Zheng L, Shang Y, Gao JH, Liu Y. Frequency dependent topological patterns of resting-state brain networks. *PLoS One* 2015;10:e0124681
15. Zuo XN, Di Martino A, Kelly C, Shehzad ZE, Gee DG, Klein DF, et al. The oscillating brain: complex and reliable. *Neuroimage* 2010;49:1432-1445
16. He BJ, Zempel JM, Snyder AZ, Raichle ME. The temporal structures and functional significance of scale-free brain activity. *Neuron* 2010;66:353-369
17. Baria AT, Baliki MN, Parrish T, Apkarian AV. Anatomical and functional assemblies of brain BOLD oscillations. *J Neurosci* 2011;31:7910-7919
18. Wang P, Li R, Yu J, Huang Z, Li J. Frequency-dependent brain regional homogeneity alterations in patients with mild cognitive impairment during working memory state relative to resting state. *Front Aging Neurosci* 2016;8:60
19. Buzsáki G, Draguhn A. Neuronal oscillations in cortical networks. *Science* 2004;304:1926-1929

20. Pugh RN, Murray-Lyon IM, Dawson JL, Pietroni MC, Williams R. Transection of the oesophagus for bleeding oesophageal varices. *Br J Surg* 1973;60:646-649
21. Atterbury CE, Maddrey WC, Conn HO. Neomycin-sorbitol and lactulose in the treatment of acute portal-systemic encephalopathy. A controlled, double-blind clinical trial. *Am J Dig Dis* 1978;23:398-406
22. Cheng Y, Huang L, Zhang X, Zhong J, Ji Q, Xie S, et al. Liver transplantation nearly normalizes brain spontaneous activity and cognitive function at 1 month: a resting-state functional MRI study. *Metab Brain Dis* 2015;30:979-988
23. Yan CG, Wang XD, Zuo XN, Zang YF. DPABI: data processing & analysis for (resting-state) brain imaging. *Neuroinformatics* 2016;14:339-351
24. Jenkinson M, Bannister P, Brady M, Smith S. Improved optimization for the robust and accurate linear registration and motion correction of brain images. *Neuroimage* 2002;17:825-841
25. Song X, Zhang Y, Liu Y. Frequency specificity of regional homogeneity in the resting-state human brain. *PLoS One* 2014;9:e86818
26. Zang Y, Jiang T, Lu Y, He Y, Tian L. Regional homogeneity approach to fMRI data analysis. *Neuroimage* 2004;22:394-400
27. Qi R, Zhang LJ, Chen HJ, Zhong J, Luo S, Ke J, et al. Role of local and distant functional connectivity density in the development of minimal hepatic encephalopathy. *Sci Rep* 2015;5:13720
28. Silk TJ, Bellgrove MA, Wrafter P, Mattingley JB, Cunnington R. Spatial working memory and spatial attention rely on common neural processes in the intraparietal sulcus. *Neuroimage* 2010;53:718-724